

Size-sensitive fractionation by high osmotic pressure chromatography using controlled pore glasses

Min Luo and Iwao Teraoka*

Department of Chemical Engineering, Chemistry, and Materials Science, Polytechnic University, 333 Jay Street, Brooklyn, NY 11201, USA

(Received 24 April 1996)

High osmotic pressure chromatography (HOPC), recently developed to separate a large amount of polydisperse polymer with respect to molecular weight, was carried out by using controlled-pore glasses (CPG) as separating media. HOPC is based on the partitioning of a polymer solution with a porous medium specific to high concentrations that exert a high osmotic pressure. The molecular weight distributions of the initial fractions separated were much narrower compared with those obtained by using silica gels, as CPG has a narrower distribution in the pore size. Furthermore, CPG with a larger pore size produced initial fractions with a higher molecular weight, thereby demonstrating that HOPC works on the basis of size exclusion even at high concentrations. The separation was optimal when the ratio of the radius of gyration of the injected polymer to the pore radius was between 1 and 2. The ratio is several times as large as the one commonly used in gel permeation chromatography © 1997 Elsevier Science Ltd.

(Keywords: liquid chromatography; size exclusion; osmotic pressure)

INTRODUCTION

Synthetic polymers are mixtures of components different in molecular weight (abbreviated hereafter as MW). Physical separation techniques such as preparative gel permeation chromatography (GPC)¹ and fractional precipitation² have been available. Their use has been limited, however, because dilute solution conditions require consumption of a large volume of solvent. To alleviate the problem, we recently proposed high osmotic pressure chromatography (HOPC)³ for large-scale separation of polymer with respect to MW. The HOPC system uses a column packed with solvent-imbibed porous materials that have a pore opening comparable to the dimension of solvated polymers. A concentrated, viscous solution of the polymer (several times as high as the overlap concentration c^* , defined as $c^*(R_g)^3 = M/N_A$, where R_g is the radius of gyration of the polymer in the dilute solution limit, M is the MW, and N_A is the Avogadro's number) is injected into the column by a high-pressure liquid pump until the polymer is detected at the column outlet. Then, the injection is switched to the pure solvent. The eluent is collected into different fractions until it returns to pure solvent. Both the concentration and volume of injection in HOPC are two to three orders of magnitude as large as those commonly practiced in GPC, thereby allowing a large processing capacity.

HOPC is based on coupling of size exclusion by a porous medium and repulsions between solvated polymer chains at high concentrations. This second factor distinguishes HOPC from GPC. The ratio of the polymer concentration in the pore to the one in the surrounding solution is called the partition coefficient K . At low concentrations (well below

c^*), K is a decreasing function of MW and $K < 1$ for any MW. GPC is based on this size exclusion principle for isolated polymer molecules. The partitioning changes, however, as the concentration c of the polymer exceeds c^* . A semidilute solution ($c > c^*$) has an osmotic pressure Π that scales as $\Pi/c k_B T \cong (c/c^*)^{5/44}$, where $k_B T$ is the thermal energy. The increased osmotic pressure drives the polymer molecules into the pores at a larger proportion, resulting in an increase in K ^{5,6}. The increase is manifested in the longer GPC retention time with increasing concentration even for $c < c^*$ ^{7–9}. Direct measurements^{10–12} and computer simulations^{13–16} also demonstrated the transition. At sufficiently high concentrations, K approaches, but does not exceed, unity. The partitioning is different when the solute is a polydisperse polymer. The osmotic pressure-driven migration favors low-MW components because of size exclusion. In contrast to the partitioning at low concentrations, K for the low-MW components easily exceeds unity, whereas K for high-MW components is smaller than it is in the absence of the low-MW components¹⁷. Note that low-MW components alone do not cause the partitioning inversion. In particular, when the pore channels and the surrounding solution have a comparable volume, the partitioning inversion leaves the exterior solution deficient in the low-MW components that occupy the volume in the pore channels with a high purity¹⁸. This segregation of the polymer by MW was formulated into an equilibrium separation scheme called enhanced partitioning fractionation^{18,19}.

HOPC essentially repeats this enhanced partitioning between the mobile phase (exterior to the pore) and the stationary phase (interior of the porous materials) as the mobile phase is transferred to the next plate³. The front end of the mobile phase that contains polymer drives low-MW

* To whom correspondence should be addressed. Tel.: +1 718 2603466; fax: +1 718 2603125.

components into the stationary phase at each plate, thereby increasing its purity of the high-MW components in the mobile phase. The first fraction of the eluent is therefore enriched with the highest MW components present in the column. The next portion of the mobile phase has to establish concentration equilibrium with the stationary phase that contains low-MW components. Removal of these components from the mobile phase is not as easy as for the front end. Thus, the average MW for later fractions decreases, and the polydispersity index M_w/M_n increases (M_w and M_n are the weight-average and number-average MWs). Collection of the eluent is continued until all of the polymer injected is recovered.

We constructed HOPC systems using silica gels as exclusion media and applied HOPC to various broad-distribution polymers³. After each separation, GPC was used to analyze the MW distribution for the fractions obtained and for the injected polymer. The polydispersity index of the initial fractions decreased typically to a square root of the index of the injected polymer. The peak MW decreased, and M_w/M_n increased for later fractions, in agreement with the predictions. Chromatograms from different batches of HOPC under similar conditions were reproducible. The loading capacity was high, typically several hundred milligrams of polymer for a column of 3.9 mm interior diameter and 300 mm length. The most significant feature of HOPC was the ability to produce a large amount of high-MW components in a narrowed distribution. We showed comparisons of HOPC separation conducted under various conditions. In particular, when the concentration was lower while the injection volume was held unchanged and when the injection volume was smaller while the concentration was held high, the performance deteriorated. HOPC worked only when it employed both high concentration and large volume injection. The other extreme is GPC that has a high resolution only when the concentration is sufficiently low and the injection volume is small.

The HOPC exhibited a resolution sufficient to separate anionically prepared polystyrene standards³. However, the resolution was not as good as expected*. Furthermore, separation using silica gels of three different nominal pore sizes (6, 9, and 15 nm) did not show a marked pore size dependence³. Silica gels with the pore diameter 15 nm separated equally well polymers of various molecular weights that range from $M_w = 4.73 \times 10^4$ of polycarbonate (with reference to polystyrene standards) to $M_w = 1.74 \times 10^6$ of a polystyrene standard. We ascribed these results partly to the broad pore size distribution in the separating media.

Separation results obtained using silica gels raise a question about the mechanism of separation in HOPC, especially the size exclusion principle. To answer this question, we carried out HOPC using controlled-pore glasses (CPG)^{20,21} that have a much narrower distribution in the pore size²² than silica gels do. The resolution of the HOPC separation improved considerably compared with the silica gels. Furthermore, the separation showed marked dependence on the pore size. From the results of separations carried out for various combinations of the pore size and chain dimension, we find a criterion to select the optimal pore size for a given polydisperse polymer.

* Model calculations were performed, assuming enhanced partitioning at every plate.

EXPERIMENTAL SECTION

Materials

Characteristics of the porous materials used in the present study are shown in Table 1. CPGs were obtained from CPG, Inc., and silica gels (Davisil®) were from Davison of W.R. Grace. The mean pore diameter d_m and the distribution δ were calculated from a plot of the cumulative pore volume as a function of the pore diameter. Let d_{10} , d_{50} and d_{90} be the diameters that give the cumulative pore volumes equal to 10, 50, and 90% of the total pore volume, respectively. Then $d_m \equiv d_{50}$, and $\delta \equiv (d_{90} - d_{10})/(2d_{50})$. The specific pore volume, v_m , is defined as the volume of pore per unit mass of silica. The bead size is the average of the upper and lower bounds of the bead size included. The tabulated data for CPGs were supplied by CPG, Inc. The pore size distribution data for silica gels were calculated from the desorption data supplied by Davison.

Chlorotrimethylsilane obtained from Aldrich, and tetrahydrofuran (THF, spectroscopy grade) purchased from EM Science were used as received. Methanol, from EM Science, was filtered before use. Table 2 lists polymer samples used in this study: poly(methyl methacrylate) (PMMA), polycaprolactone (PCL), poly(hexyl isocyanate) (PHIC), and polystyrene (PS). Empty stainless steel columns were purchased from Phenomenex. To minimize adsorption of polymer molecules onto the pore walls, the surface silanol groups of silica were replaced by trimethylsilanol groups as described elsewhere³.

Instrumentation

A high osmotic pressure chromatography (HOPC) system consists of a column packed with surface-treated porous silica, a high-pressure liquid pump, a fraction collector (Eldex, Model 1243) with a drop counter, and a UV-visible detector (Alltech, Model 450 UV, 254 nm). Columns used have a dimension of interior diameter, i.d., of 3.9 mm and length of 300 mm. Prior to injection of the polymer solution in each batch of HOPC, the column was washed with the same solvent that was used to dissolve the polymer. A

Table 1 Characteristics of the porous glasses

Porous glass	Code	d_m (nm) ^a	δ (%) ^a	v_m (ml/g) ^a	Bead size (μm)
Silica gel	Grade 642	13.9	24 ^b	1.15	37
CPG	CPG 75C	8.1	9.0	0.49	52
CPG	CPG 120Ca	12.8	5.1	0.80	52
CPG	CPG 120Cb	13.0	7.4	0.68	52
CPG	CPG 240Ca	25.3	6.1	0.49	52
CPG	CPG 240Cb	24.2	3.9	0.89	52
CPG	CPG 240Cc	24.2	4.9	0.96	52
CPG	CPG 350C	34.3	5.0	0.97	52

^aSee text for definition.

^bCalculated from the desorption data.

Table 2 Characteristics of the polymers

Polymer	Source	M_w^a	M_n^a
PMMA 130K	Aldrich	7.87×10^4	3.97×10^4
PMMA 670K	Aldrich	4.73×10^5	1.67×10^5
PCL 20K	Aldrich	2.53×10^4	1.55×10^4
PCL 120K	Aldrich	1.31×10^5	9.20×10^4
PS 280K	Aldrich	2.86×10^5	1.46×10^5
PHIC	Polysciences	3.93×10^5	1.58×10^5

^aPolystyrene-equivalent molecular weight.

concentrated solution of the polymer and the solvent were injected from a vial into the column through the pump at 0.10 ml/min. We collected ca. 30 drops of the eluent in each of the initial fractions (typically fractions 1–5), 50 drops in the intermediate fractions (6–13), and 150 drops in the later fractions. All of the HOPC processing was performed at room temperature. Polymer was precipitated by adding excess methanol and then dried in vacuum. The detector produced a non-zero signal even when the polymer was UV insensitive. Nonuniform distribution of the refractive index in the flowcell is considered to have decreased the intensity of the transmitted light.

Analysis of molecular weight

The MW distribution for the fractions collected and the original polymer was analyzed by using a Waters analytical GPC system with a Model 510 HPLC pump and a Model 410 differential refractometer. A set of three columns (Phenogel, Phenomenex) of sizes 10^3 , 10^4 , and 10^5 Å were used (35°C). The mobile phase was THF, and the flow-rate was 1.0 ml/min. The analytical columns were calibrated with polystyrene standards (Pressure Chemical) of MW from 1.36×10^4 to 2.16×10^6 . All of MWs given in this contribution are with reference to polystyrene.

RESULTS AND DISCUSSION

Dependence on the separation media

We carried out an HOPC separation using a column packed with CPG 120Ca for a 25.0 wt.% solution of PMMA 130K ($M_w = 7.87 \times 10^4$, $M_w/M_n = 1.98$) in THF to compare the performance with that of silica gels reported earlier³. The two packing materials have a similar mean pore diameter, but the distribution is much broader in silica gels (Table 1). The amount of injection was 2.10 and 2.04 g for the CPG and silica gel columns, respectively. A total of 13 fractions was collected for each of two columns. The amount of polymer recovered in the same number of fractions was similar between the two columns. Some of the chromatograms for the separated fractions are shown in

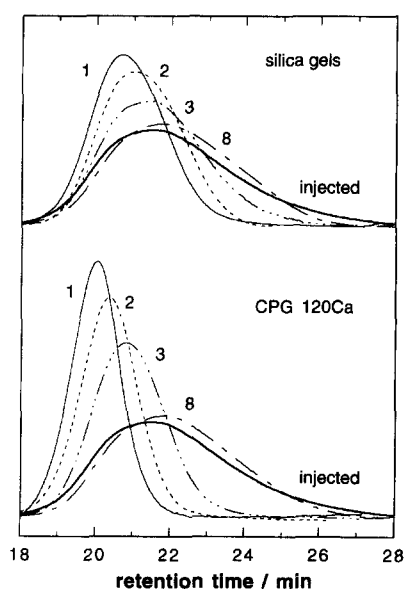


Figure 1 GPC chromatograms for the injected polymer PMMA 130K ($M_w = 7.87 \times 10^4$, $M_w/M_n = 1.98$) (thick solid lines) and for fractions 1, 2, 3, and 8 obtained in HOPC. The separation media were silica gels and CPGs that have a similar mean pore diameter

Figure 1, together with a chromatogram of the injected polymer. For separation by the silica gels we re-analyzed the fractions obtained earlier³. Each chromatogram is normalized by the area. The separation by the CPG produced fractions with a narrower distribution than the separation by silica gels, especially for initial fractions. For fraction 1, M_w/M_n dropped to 1.15, about 1/5 power of 1.98, the index of the original sample. In contrast, silica gels decreased the index to 1.27 for fraction 1. The improved separation performance for pores with a narrower distribution indicates that HOPC uses size exclusion principles even at high concentrations.

Pore size dependence

Columns packed with CPG 120Ca, 240Cb, and 350C ($d_m = 12.8$, 24.2, and 34.3 nm, respectively) were used to separate PMMA 670K ($M_w = 4.73 \times 10^5$, $M_w/M_n = 2.83$). At M_w of the original sample, the radius of gyration R_g of the polymer is estimated to be 29.7 nm, assuming that the GPC retention time is a function of R_g and using an empirical formula $R_g = 0.0125 \times M_w^{0.595}$ obtained for polystyrene in good solvent²³. A 12.0 wt.% solution of the polymer in THF was injected. The amounts of the polymer solution injected were 1.87, 1.82, and 1.74 g, respectively. A total of 14, 14, and 15 fractions was collected in each separation. The chromatograms of the fractions separated by using CPG 120Ca and 240Cb are shown in Figure 2. Fraction 1 from CPG 120Ca has an elution curve similar to that of fraction 2, and is not shown. The larger pore produced initial fractions with a shorter peak retention time. In later fractions, the smaller pore outperformed the other, collecting fractions purer in the low-MW components, although the resolution was not good.

Figure 3 shows M_w/M_n as a function to M_w for fractions obtained in the three separations including those shown in Figure 2. The larger pore produced initial fractions with a higher M_w , but the amount recovered was less. In HOPC,

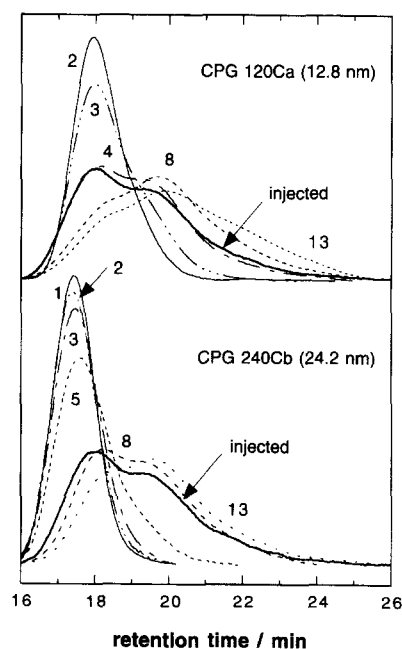


Figure 2 GPC chromatograms for the injected polymer PMMA 670K ($M_w = 4.73 \times 10^5$, $M_w/M_n = 2.83$) (thick solid lines) and for fractions obtained in HOPC. Two sets of fractions were obtained in two HOPC batches using CPG-filled columns that have different mean pore diameters, 12.8 and 24.2 nm.

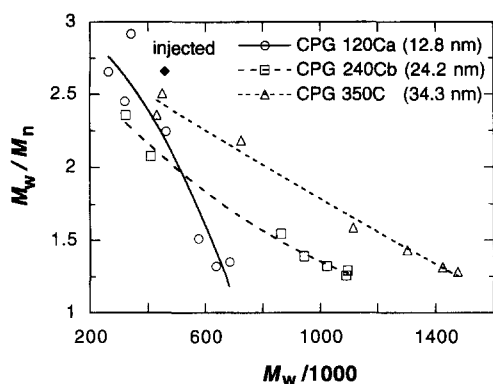


Figure 3 Polydispersity index M_w/M_n as a function of M_w for fractions obtained from PMMA 670K in HOPC separation using three CPG-filled columns with different pore diameters, 12.8, 24.2, and 34.3 nm

low-MW components are preferentially driven into pore channels by the high osmotic pressure of a concentrated solution. When the pore size is too large, only the highest-MW components will be partitioned in the mobile phase. Therefore, M_w values in the initial fractions, obtained with the 34.3-nm pore, are high, and the amounts recovered are small. In contrast, when d_m was as small as 12.8 nm, less than half of R_g at M_w of PMMA 670K, a large proportion of polymer, including relatively low-MW components, was partitioned in the mobile phase. Therefore, the initial fractions had a broad distribution and a small M_w . The pore size dependence indicates that the separation uses size exclusion.

If HOPC's principle is segregation driven by the high osmotic pressure, an increase in the concentration of the injected polymer solution will result in a more preferred partitioning of the polymer in the stationary phase, even with the smallest pore of the three. Then the mobile phase will be more deficient in low-MW components for the initial fractions. To see the effect of the concentration, we prepared a highly viscous 16.0 wt.% solution of PMMA 670K in THF and injected it into the column packed with CPG 120Ca. Compared with the 12.0 wt.% solution shown in Figure 3, M_w increased in initial fractions, as expected. The polydispersity was larger, however, probably because slower diffusion of highly entangled polymer chains at high concentrations required a longer equilibration time and therefore the mobile phase was transferred to the next plate before equilibration. We observed similar concentration dependence in the HOPC separation using silica gels³.

We also studied the pore size dependence for a 25.0 wt.% solution of PMMA 130K ($R_g \cong 10.2$ nm at M_w) in THF. The solution, 1.97, 2.06, and 2.28 g, was injected into columns packed with CPG 75C, 240Ca, and 350C ($d_m = 8.1, 25.3,$ and 34.3 nm, respectively). Figure 4 shows M_w/M_n as a function of M_w for the three separations. The separation by CPG 120Ca ($d_m = 12.8$ nm) shown in Figure 1 is included here for reference. Compared with CPG 240Ca, CPG 120Ca generated a higher M_w in the initial fractions, a broader span of M_w , and in general a smaller M_w/M_n . When the pore size is too large, as in CPG 240Ca, a larger proportion of the polymer chains are included in the pore channels, resulting in a poorer separation. The situation is even worse with CPG 350C. When the pore size is too small as with CPG 75C, however, M_w of the initial fractions was again smaller compared with that for CPG 120Ca. Unlike the separation of PMMA 670K, the smallest pore did not outperform the others in the separation of the later fractions. We find this

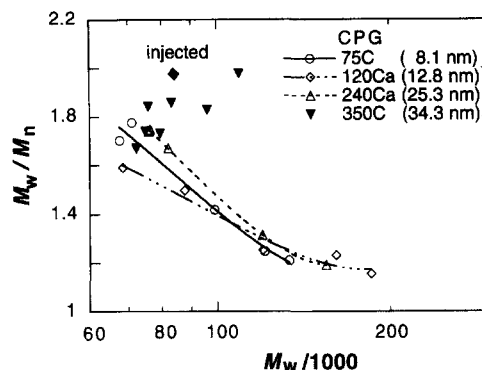


Figure 4 Polydispersity index M_w/M_n as a function of M_w for fractions obtained in HOPC separation of PMMA 130K. The separation media were CPGs with mean pore diameters of 8.1, 12.8, 25.3, and 34.3 nm, respectively

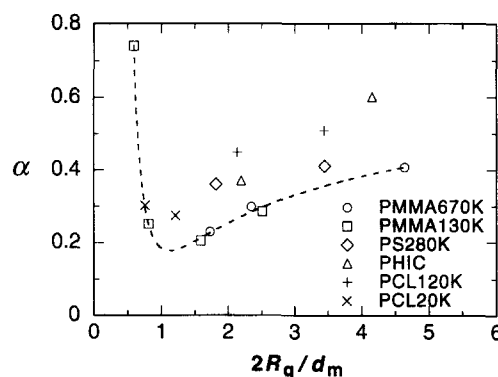


Figure 5 Exponent α as a function of $2R_g/d_m$ for the fractions obtained in HOPC separation of PMMA 670K, PMMA 130K, PS 280K, PHIC, PCL 120K, and PCL 20K. See text for definition of α

problem is specific to CPG 75C and discuss it below together with separations of other polymers.

To quantify narrowing in the MW distribution of the initial fraction, we introduce an exponent α defined by $[(M_w/M_n)_0]^\alpha = (M_w/M_n)_1$, where $(M_w/M_n)_0$ and $(M_w/M_n)_1$ are the polydispersity indices of the injected sample and the initial fraction, respectively. A smaller α denotes a better resolution. Figure 5 shows a plot of α as a function of $2R_g/d_m$, where R_g is the radius of gyration at M_w of the injected polymer. Results compiled from the separations of PMMA 670K and PMMA 130K with various CPGs are shown, along with those for PHIC, PS 280K, PCL 120K, and PCL 20K. As the separation performance depends on the concentration of the polymer solution, $(M_w/M_n)_0$, and the number of drops collected in the first fraction, plots in Figure 5 should be considered to bear a vertical error bar of ca. 0.1. PMMA 670K with three pore sizes and PMMA 130K with four pore sizes combined encompass a broad range of the polymer dimension to pore size ratios. The values of α for a different $2R_g/d_m$ appear to lie on a master curve indicated by a dashed line. Selection of pores with $1 < 2R_g/d_m < 2$ gives the optimal narrowing for the initial fraction. Note that, in separations using silica gels, α was around 0.5 for the similar range of $2R_g/d_m$. We will discuss results for other polymers below.

A random coil polymer and a semi-rigid polymer exhibit different solution thermodynamics. We are concerned here if the chain dimension estimated from the GPC retention time gives an estimate of the optimal pore diameter for the separation of the semi-rigid polymer. The polymer we

separated is PHIC ($M_w = 3.93 \times 10^5$, $M_w/M_n = 2.49$) that has a persistence length of 30–40 nm²⁴. We used columns packed with CPG 120Cb ($d_m = 13.0$ nm) and CPG 240Cc ($d_m = 24.2$ nm). An 8.0 wt.% solution of PHIC in THF was injected. The amount was 1.61 and 1.67 g, respectively. The performance of CPG 240Cc was better. The M_w values of its first three fractions were higher than those from the other column with the smaller d_m . The fractions from CPG 240Cc encompassed a broader range of M_w and had a smaller M_w/M_n in the entire range of M_w . The better result with CPG 240Cc is in agreement with what we observed for the separation of PMMA 670K. Note that PHIC and PMMA 670K have a similar polystyrene-equivalent MW. The R_g estimated from the GPC retention time provides a criterion for the selection of the optimal pore diameter. In Figure 4, α of PHIC is located above the master curve for PMMA, which we ascribe to the chain rigidity. The partition coefficient of a rigid chain has a more gradual dependence on R_g than that of a flexible chain^{25–27}. Therefore, the resolving power with respect to R_g is weaker for rigid chains.

In analytical GPC, the optimal range of the pore size for a given polydisperse polymer is approximately $1/4 < 2R_g/d_m < 1/2$ ²⁸. GPC often uses mixed-bed columns that have a distribution in the pore size to provide a linear relationship between the retention time and log(MW). In HOPC, in contrast, use of pores of a single pore size is necessary, and the pore size needs to be much smaller than the one appropriate for GPC. HOPC deliberately uses small pores that exclude nearly all MW components at low concentrations but allows entry of low MW components only at elevated concentrations by the high osmotic pressure. Use of the same pore size as used in GPC results in a poor separation as seen in Figure 4 for PMMA 130K with CPG350C. The latter is essentially an overloading in GPC.

The narrow pore size distribution of CPG resulted in a pronounced size selectivity. Table 1 shows that CPG 75C has a broader distribution than other CPGs with a larger pore size. Size selection by CPG 75C is expected not to be as effective as other grades of CPG. We compared the performance of columns packed with CPG 120Cb and CPG 75C for a 25.0 wt.% solution of PCL 120K and a 40.0 wt.% solution of PCL 20K in THF. The M_w of the initial fraction from CPG 120Cb was slightly higher than that obtained from CPG 75C for each of the two polymer solutions, a reasonable result if we take into account the larger pore size of CPG 120Cb. However, the difference was small, and the span of M_w and values of M_w/M_n were similar. Unlike in Figures 2 and 3, the smaller pore did not excel in narrowing the distribution for later fractions. We ascribe these results to the broader pore size distribution of CPG 75C. Presence of large pores in CPG 75C is considered to have allowed collection of fractions with a large M_w in the initial fractions. We also note that later fractions of PCL 20K showed a narrower MW distribution, although the amount of the polymer recovered was small compared with earlier fractions. This tendency was not seen in polymers with a higher M_w in any columns. The narrower distribution in later fractions is in agreement with a model calculation*. In Figure 5, α of PCL (for both samples) is located above the master curve for PMMA. We consider that the narrowing of M_w was not significant because $(M_w/M_n)_0$ was already small.

* Model calculations were performed, assuming enhanced partitioning at every plate.

CONCLUDING REMARKS

We have shown that use of CPGs improved the resolution of HOPC compared with the separation using silica gels reported earlier³. The difference is due to a narrower distribution of pore size in CPGs. By the same reason, the pore size dependence was more significant than the one we observed with silica gels. The optimal pore size for HOPC was found to be much smaller than the size commonly used in GPC. These results are in good agreement with the proposed mechanism for the HOPC separation that coupling of size exclusion by the pore and a high osmotic pressure of the concentrated solution effects the separation.

CPGs have a network structure of pores that resemble a cylindrical pore only over a short distance comparable to the pore diameter. A polymer chain at a junction of these pores has a smaller free energy than the chain in the cylinder portion of the pore. The pore size distribution, in terms of cylinder-equivalent pore diameter, will be much broader than the distribution estimated in the mercury porosimetry. Use of a confining medium comprising cylindrical pores with uniform radius will further improve the resolution. These media include nano-channel array glasses²⁹ and meso-porous silicates³⁰ produced by sintering of columnar packing of silicon-containing surfactant molecules.

ACKNOWLEDGEMENTS

Partial support by ACS Petroleum Research Fund and NSF Young Investigator Award is gratefully acknowledged. We also thank Dr. H. Wechsler for financial support.

REFERENCES

1. Yau, W.W., Kirkland, J.J., Bly, D. D., Modern Size Exclusion Liquid Chromatography, John Wiley, London, 1979.
2. Bello, A., Barrales-Rienda, J.M., Guzman, G.M., in Polymer Handbook, 3rd edn, ed. J. Brandrup, E.H. Immergut, John Wiley, New York, 1989.
3. Luo, M. and Teraoka, I., *Macromolecules*, 1996, **29**, 4226.
4. de Gennes, P.G., Scaling Concepts in Polymer Physics, Cornell University Press, Ithaca, 1979.
5. Daoud, M. and de Gennes, P.G., *J. Phys. (Paris)*, 1977, **38**, 85.
6. Teraoka, I., Langley, K.H. and Karasz, F.E., *Macromolecules*, 1993, **26**, 287.
7. Bleha, T., Mlnek, J. and Berek, D., *Polymer*, 1980, **21**, 798.
8. Bleha, T., Spychaj, T., Vondra, R. and Berek, D., *J. Polym. Sci. Polym. Phys. Ed.*, 1983, **21**, 1903.
9. Boehm, R.E., Martire, D.E., Armstrong, D.W. and Bui, K.H., *Macromolecules*, 1984, **17**, 400.
10. Satterfield, C.N., Colton, C.K., Turckheim, B.D. and Copeland, T.M., *AIChE J.*, 1978, **24**, 937.
11. Brannon, J.H. and Anderson, J.L., *J. Polym. Sci. Polym. Phys. Ed.*, 1982, **20**, 857.
12. Teraoka, I., *Macromolecules*, 1996, **29**, 2430.
13. Cifra, P., Bleha, T. and Romanov, A., *Polymer*, 1988, **29**, 1664.
14. Cifra, P., Bleha, T. and Romanov, A., *Macromol. Chem. Rapid Commun.*, 1988, **9**, 355.
15. Bleha, T., Cifra, P. and Karasz, F.E., *Polymer*, 1990, **31**, 1321.
16. Thompson, A.P. and Glandt, E.D., *Macromolecules*, 1996, **29**, 4314.
17. Teraoka, I., Zhou, Z., Langley, K.H. and Karasz, F.E., *Macromolecules*, 1993, **26**, 3223.
18. Teraoka, I., Zhou, Z., Langley, K.H. and Karasz, F.E., *Macromolecules*, 1993, **26**, 6081.
19. Dube, A. and Teraoka, I., *Macromolecules*, 1995, **28**, 2592.
20. Haller, W., *Nature*, 1965, **206**, 693.
21. Haller, W., in Solid Phase Biochemistry, ed. W.H. Scouten, John Wiley, New York, 1983, pp. 535–597.
22. Schmidt, P. W., in Characterization of Porous Solids, Vol. 39, ed. K.K. Unger, J. Rouquerol, K.S.W. Sing, H. Kral, Elsevier Science Publishers B.V., Amsterdam, 1988, p. 35.

Size-sensitive fractionation: M. Luo and I. Teraoka

23. Huber, K., Bantle, S., Lutz, P. and Burchard, W., *Macromolecules*, 1985, **18**, 1461.
24. Itou, T., Chikiri, H., Teramoto, A. and Aharoni, S.M., *Polym. J.*, 1988, **20**, 143.
25. Davidson, M.G., Suter, U.W. and Deen, W.M., *Macromolecules*, 1987, **20**, 1141.
26. Priest, R.G., *J. Appl. Phys.*, 1981, **52**, 5930.
27. Teraoka, I., *Prog. Polym. Sci.*, 1996, **21**, 89.
28. Haller, W., *Macromolecules*, 1977, **10**, 83.
29. Tonucci, R.J., Justus, B.L., Campillo, A.J. and Ford, C.E., *Science*, 1992, **258**, 783.
30. Kresge, C.T., Leonowicz, M.E., Roth, W.J., Vartuli, J.C. and Beck, J.S., *Nature*, 1992, **359**, 710.